RASĀYAN *J. Chem.*
Vol. 16 | No. 3 |1435-1443| July - September | 2023
ISSN: 0974-1496 | e-ISSN: 0976-0083 | CODEN: RJCABP
http://www.rasayanjournal.com
http://www.rasayanjournal.co.in

COORDINATION BEHAVIOUR AND COMPUTATIONAL STUDIES OF 3-FORMYL CHROMONE N(4)-METHYL-N(4)-PHENYLTHIOSEMICARBAZONE AND ITS TRANSITION METAL COMPLEXES

K. G. Sangeetha[1,✉] and K. K Aravindakshan[2]
[1]Department of Chemistry, The Zamorin's Guruvayurappan College,
Calicut, 673014, Kerala, India
[2]Department of Chemistry, University of Calicut, 673635, Kerala, India
✉Corresponding Author: sangtkg@gmail.com

ABSTRACT

This article reports on the 3-formylchromone N(4)-substituted thiosemicarbazone's coordination behavior towards transition metal ions. CHNS analysis, magnetic moment, thermal analysis, IR, UV, NMR, and EPR spectroscopy were used to characterize the compounds. Moreover, DFT, insilico ADME, and docking studies of the ligand were done. Based on the spectral results, copper, cobalt, and nickel complexes had square planar geometry. Conversely, the manganese complex has octahedral geometry. The Gaussian 09 program is utilized for DFT studies. The GLIDE program was used for docking calculations. As receptor molecules, histone deacetylase, ribonucleotide reductase, and DNA methyltransferase were chosen. The SwissADME tool was used to evaluate the pharmacokinetics of the ligand. Based on Lipinski's rules, the estimation of insilico ADMET discovered that ligands procure significant drug-likeness characteristics. Its ability to block histone deacetylase 8 (PDB ID 1T69) protein is shown by docking calculations, and its proper action can be further confirmed in wet lab tests.

Keywords: DFT, Molecular Docking, Ribonucleotide Reductase, Histone Deacetylase 8, DNA Methyl Transferase.
RASĀYAN *J. Chem.*, Vol. 16, No.3, 2023

INTRODUCTION

Thiosemicarbazones are one of the most dynamic frameworks found in a wide range of biologically active compounds. The biological activities of thiosemicarbazones may be due to the presence of sulphur atoms. They are gaining popularity in antitumor, antiprotozoal, antibacterial, and antiviral research. Their action in all of these cases includes interaction with metal ions.[1,2]These compounds are the first to be found in clinical medicine for viral diseases and to be effective in humans. 3-aminopyridine-2-carboxaldehyde thiosemicarbazone, an anticancer drug has progressed to clinical phase II for a variety of cancer types.[3,4] By the way, metal complexes of 3-formylchromone Schiff bases have numerous applications in biological, clinical, and pharmacological areas, including antimycobacterial, antifungal, anticonvulsant, antimicrobial, and mushroom tyrosinase inhibition activity.[5,6,7,8] Some are used as cisplatin alternatives in cancer treatment.[9]Metal complexes of chromone hydrazones frequently exhibit numerous biological and pharmaceutical actions, such as antibacterial, antituberculostatic, anticancer, and antioxidant properties.[10,11,12] DNA binding studies of chromone Schiff bases and their metal complexes[13] are well supported by the literature. We were fascinated with the properties of these compounds, and we tried to combine substituted thiosemicarbazide with 3-formyl chromone expecting more biological properties. Existing pharmaceutical R&D has been a high-threat investment and increasing productivity has always been a major concern for the pharmaceutical industry. To solve this problem, several multidisciplinary methodologies, such as structural biology, computational chemistry, and information technology are required for the process of drug development.[14]It has been reported that the widespread usage of computational techniques could cut drug development costs by up to 50%.[15] It would be impractical to conduct elaborate and expensive ADME/T experimental methods, *in silico* ADME/T calculation is fetching the means of choice in drug discovery. Cancer treatments are now aimed at inhibiting the growth of cancer cells using a cell cycle-based mechanism that mimics the body's natural process.[16] This method does not

http://doi.org/10.31788/RJC.2023.1638352
This work is licensed under a CC BY 4.0 license.

damage ordinary cells as well as reduces the combined side effects caused by chemotherapy. Inhibiting histone deacetylases (HDAC), ribonucleotide reductase, and DNA methyl transferase enzymes have emerged as a novel cancer treatment strategy.[17,18,19] HDAC inhibitor interacts with cancer cell chromosomes and inhibits cell growth. The R2 subunit of ribonucleotide reductase regulates the enzyme's catalytic activity to provide DNA synthesis *via* reduction. DNA methyl transferases are important parts of larger complexes that are involved in modulating chromatin structure and controlling transcription, etc.[20,21,22] Abnormal DNA methylation patterns also contribute to the development of cancer. With this in mind, we synthesized novel 3-formyl chromone N(4)-methyl-N(4)-phenyl thiosemicarbazone and its transition metal complexes and insilico ADME, molecular docking are presented here.

EXPERIMENTAL

CHNS analyses were carried out using the Vario EL III elemental analyzer. KBr pellet was used to generate IR spectra on a Jasco-FT-IR-4100 model spectrometer. The electronic spectra were recorded on a JascoV-550 UV-Vis spectrometer. 400 MHz Bruker NMR spectrometer was used to record ^{1}H NMR spectra. At room temperature, the magnetic moment for the complexes was calculated using Sherwood Scientific Magnetic Susceptibility Balance. TGA Q50 V20.13 Build 39 model thermogravimetric analyzer fitted with a thermal analysis controller was used to measure TG/DTG in a nitrogen atmosphere with a heating rate of 10^{o}C/min. 3-formylchromone N(4)-methyl-N(4)-phenyl thiosemicarbazone was prepared by the procedure reported earlier9.[9] The compound was obtained as yellow solids, filtered, washed with methanol, and dried. The reaction route in the synthesis of the ligand is presented in Scheme-1

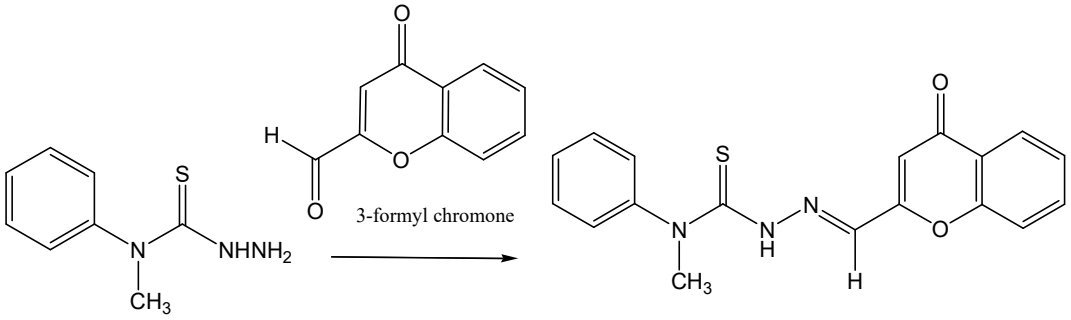

MPTSC FMPTSC

Scheme-1: Synthetic Route of the Ligand Formation

The preparation of metal complexes is achieved by adding the hot metal salt solution dropwise into the hot methanolic ligand solution. The reaction mixture was stirred and refluxed at room temperature for 60 min. The colored complex was isolated from the reaction media, washed several times with water and methanol, dried, and kept in a desiccator.

Computational Studies

The initial geometry of the molecule was created using GAUSS-VIEW 5.0.9 program.[23] The compound was optimized at Becke's three-parameter hybrid exchange functional and the Lee-Yang-Parr non-local correlation functional (B3LYP) level in the ground state.[24,25] Frontier molecular orbitals and the MEP map of the compound were produced by using the optimized structures. We determined the ADME (Absorption, distribution, metabolism, excretion) description of the compound using the SWISSADME web tool. Five predictive models are offered, including iLOGP, XLOGP, WLOGP, MLOGP, and SILICOS-IT, to calculate the molecule's lipophilicity based on its partition coefficient between n-octanol and water.[26] In order to evaluate solubility, three topological methods Esol model, Ali model, and SILICOS-IT are offered. Drugs are absorbed depending on their membrane permeability shown by colon cancer cell line (Caco-2)], intestinal absorption, skin permeability levels, P-glycoprotein substrate, or inhibitor. The drug distribution can be determined by the blood-brain barrier (logBB), CNS permeability, and volume of distribution (VDss). Metabolism is determined by the CYP models for substrate or inhibition (CYP2D6, CYP3A4, CYP1A2, CYP2C19, CYP2C9, CYP2D6, and CYP3A4).40[40] Oral bioavailability, ADME, drug-likeness,

and medicinal chemistry friendliness are authenticated by Lipinski's Rule of Five.[27] Using the GLIDE Dock Program, the compound was docked into the 3D crystal structures of DNA methyltransferase, histone deacetylase 8, and ribonucleotide reductase M-2 component (PDB ID: 1T69, 2QRV, and 2UW2, respectively). Heavy atoms were restrained using Impref minimization, which can be done using the OPLS 2005 force field, and protein structure was optimized using the protein preparation wizard, which uses restrained minimization[28,29,30].To prepare ligands, the Maestro interface (9.0) of the Schrodinger software was utilized, specifically the ligand preparation wizard (Lprep).[30] The active site's grid center is specified, and box sizes are configured to be 15 Å. By taking note of the interaction energy between the ligand and the protein, the optimal position was determined. Utilizing XP visualization, glide score and glide energy were examined.[30]

RESULTS AND DISCUSSION

Characterization of the Ligand

Yield; 80%, mp 170°C; Found : C 64.4; H 4.4; N 12.5; S 9.4; $C_{18}H_{15}N_3O_2S$. calculated: C 64.1; H 4.4; N 12.5; S 9.5 % .UV(solid, λ_{max}/ nm): 259, 321, 385nm. IR (KBr ν_{max}/cm^{-1}): ν(NH) 3426–3487, ν(C=O) 1642, ν(C=N) 1572, ν(C=S) 794; ^{1}H NMR: (DMSO) *δppm* 11.423, *δ* 8.05 *(*1H, s), *δ* 7.2 - 7.9 (10H, m), 3.612(3H, s) Fig.-S1

Characterization of Metal Complexes

In complexes, the ligand acts as tridentate, monoanionic, or neutral forms. Based on partial elemental analyses, and magnetic, thermal, and spectral observations, we have assigned the formula $MLX(H_2O)_n$ for complexes (1, 2, 3, 5, and 6) which is tabulated in Table-1.

Table-1: Microanalytical Data of Complexes

Compound	M.W.	M.P.	Colour	Yield	Elemental analysis found(calculated)					μ in BM
					C	H	N	S	M	
$C_{18}H_{15}N_3O_2S$	337	170	Yellow	80	64.4 (64.1)	4.4 (4.4)	12.5 (12.5)	9.4 (9.5)	_	_
Mn(L)OH $(H_2O)_2$ **1**	444	240	brownish black	70	48.5 (48.6)	4.3 (4.3)	9.5 (9.5)	7.3 (7.2)	12.0 (12.0)	4.80
Co(L)OH $4H_2O$ **2**	485	>260	Brown	80	44.3 (44.4)	4.8 (4.7)	8.7 (8.7)	6.6 (6.6)	12.0 (12.1)	2.58
Ni(L)Cl.H_2O **3**	448	200	light green	70	48.3 (48.2)	3.7 (3.8)	9.2 (9.3)	7.3 (7.2)	13.5 (13.6)	D
CuLCl.H_2O **4**	456	220	Green	80	47.4 (47.5)	3.6 (3.7)	9.7 (9.6)	7.2 (7.3)	14.2 (14.0)	1.45
Cd(L)Cl.$2H_2O$ **5**	520	235	Golden	70	41.2 (41.4)	3.4 (3.5)	8.3 (8.1)	6.3 (6.5)	21.6 (21.4)	D

Spectral Analysis

As we were unable to succeed in producing single crystals, we used a spectroscopic approach to elucidate the molecular structure of ligands and complexes. The IR spectrum displayed a prominent absorption band in the range 3426–3487 cm^{-1} corresponding to ν(N-H). The evidence of oxygen coordination of the carbonyl group in all the complexes is indicated by the shifting of the stretching band by 20-30 cm^{-1} from 1642 cm^{-1}. Similarly, ν(C=N) stretching vibrations of ligand get shifted to 16–39 cm^{-1} in complexes from 1572 cm^{-1}. The peak at 794 cm^{-1} due to C=S is not found in their complexes indicating the involvement of thiol sulphur.[30]The appearance of broadband around 3400 cm^{-1} in the spectra of complexes may be due to υ (OH) of water molecules.[31,32,33] The chelating mode was endorsed by the formation of two new bands in the far infrared region of the complexes around 430 and 520-568cm^{-1} that are assigned to the υ(M-N) and υ(M-O) vibrations respectively.[34] The electronic spectra help us to identify the geometry of the metal complexes. The bands observed below 350 cm^{-1} can be assigned to π→π* and n→π* transitions. Mn(II) complex exhibited two very low intense bands. One broadband at 24630 cm^{-1} due to $^6A_{1g} \rightarrow {}^4A_{1g}$(G) and $^6A_{1g} \rightarrow {}^4E_g$ (G) and another at 14556 cm^{-1} due to $^6A_{1g} \rightarrow {}^4T_{1g}$(G). This is consistent with the octahedral geometry. Square planar complexes of Co(II) give rise to two absorption bands corresponding to $^2A_1 \rightarrow {}^2E$ at higher energies and $^2A_1 \rightarrow {}^2B_1$ at lower energy regions. In the present study, we got a broad band at

24752cm^{-1} for complex **2** that can be assigned to $^2A_1 \rightarrow {}^2E$ transition and is characteristic of square planar geometry. In the Ni(II) complex, a band at 16207 cm^{-1} may be assigned to the $^1A_{1g} \rightarrow {}^1B_{1g}$ transition. Since thiols can cause spin pairing than thioethers, coordination occurs through the thiolato sulfur atom by deprotonation and not through the thioether sulfur in Ni(ll)complex and was square planar. Square planar or distorted octahedral complexes normally absorb in the region 10000-20000 cm^{-1}. The Cu(II)complex displayed a band at 16778 cm^{-1} and another at 14204 cm^{-1}. This can be assigned to $^2B_{1g} \rightarrow {}^2E_g$, $^2B_{1g} \rightarrow {}^2A_{1g}$, so we proposed a square planar geometry. The ^{1}H NMR spectrum of the Nickel(II) complex was recorded in acetone at room temperature. (Fig.-S2) A peak observed at 11.423 ppm in the ligand spectrum due to the NH proton was shifted to 11.834 ppm in the complex. This slight shift in the peak position may be due to the difference in the solvent used. A singlet observed at 8.763 ppm can be assigned to the azomethine proton. N-CH_3 protons absorb in the region 3.888 ppm. Aromatic protons show a multiplet peak in the region 6.977-7.827 ppm. The peak observed in the region, 1.980-2.089 ppm may be due to the solvent (acetone). The ESR spectrum of Cu(II) complex at 77 K in DMF was recorded in the X-band with 100 kHz field modulation Fig.-S3. Three superhyperfine lines in the perpendicular area of the spectrum indicated the coordination of azomethine nitrogen to the metal center and were caused by the interaction of the electron spin with the nuclear spin of nitrogen. We can determine that the compound is monomeric because there isn't a half-field signal. The magnetic moment explains the electronic state of the metal in the complexes. Schiff base complexes of high spin Mn(II) are found to be significantly low than the expected spin-only value and it ranges from 4.7-5.5 B.M at room temperature.[35,36] In the present investigation, the magnetic moment of complex **1** is 4.8 B.M. Square planar Co(II) complexes are of low spin, and the magnetic moment is in the range of 2.20-2.90.[37] The magnetic measurement of the Co(II) complex reported herein is 2.58 B.M. The magnetic moment of the Cu(II) complex showed a magnetic moment of 1.45 B.M. These low magnetic moments may be ascribed to significant antiferromagnetic interaction between copper centers of the complex.[38,39] The complexes of nickel, zinc, and cadmium showed diamagnetic behavior.

Thermal Studies

Thermo gravimetric analysis of Schiff base ligands and complexes is used to propose the general scheme for the thermal decomposition of metal complexes. The (NiClL)H_2O complex has undergone two stages of decomposition and is evident from the DTG peak at 150 and 260 °C. A residual mass of 30 % was left which may be due to the formation of NiS and HCl (calc.29.5 %). The complex Cu(L)Cl.H_2O, registered the first stage of decomposition between 100-150 °C with a weight loss of 4% may be due to the presence of one water molecule in the lattice. The next step of decomposition occurs in the temperature range of 180-450°C with a mass loss of 63% due to the decomposition of ligand moiety. It is evident from DTG curve peaks with temperature maxima at 145°C and 283°C. A residual mass of 25.6 % was left which may be due to the formation of CuO and HCl. The cadmium complex showed two stages of decomposition in the temperature range of 150-170°C, demonstrating the presence of lattice water molecules. DTG analysis shows two peaks at 153 and 298°C. A residual mass of 25 % was left which may be due to the formation of CdO (calc.24.6 %).

Computational Studies of 3-formylchromone N(4)-methyl-N(4)-phenylthiosemicarbazone

The optimized molecular structure, HOMO-, LUMO- and MEP plots of ligand have been generated at B3LYP/6-31+G(d,p) using the GAUSS-VIEW 5.0.9 program and are shown in Fig.-1, 2, and 3. LUMO performs as an electron acceptor while HOMO is the donor. The energy gap between the highest occupied molecular orbital and the lowest unoccupied molecular orbital is found to be 3.29 ev. The escaping tendency of electrons from an equilibrium system is described by its chemical potential while the electrophilicity index measures the stabilization in energy after a system accepts an additional amount of electronic charge from the environment.[16] By knowing the energy values of HOMO and LUMO, the global descriptive parameters of the compound can be calculated using Koopman's theorem A= $-E_{LUMO}$, I = $-E_{HOMO}$, Chemical hardness $\eta = (I - A)/2$, Chemical softness $\zeta = 1/2\eta$, Chemical potential $\mu = (E_{LUMO} + E_{HOMO})/2$, Global electrophilicity index $\omega = \mu^2 / 2\eta$[16] and is indicated in Table 2. Moreover, the MEP shows the positive potential sites around the lone pairs of sulfur and oxygen atoms projecting them as susceptible sites for the electrophilic attack.[30] The blue regions indicate the sites which are susceptible to nucleophilic attack.[38]

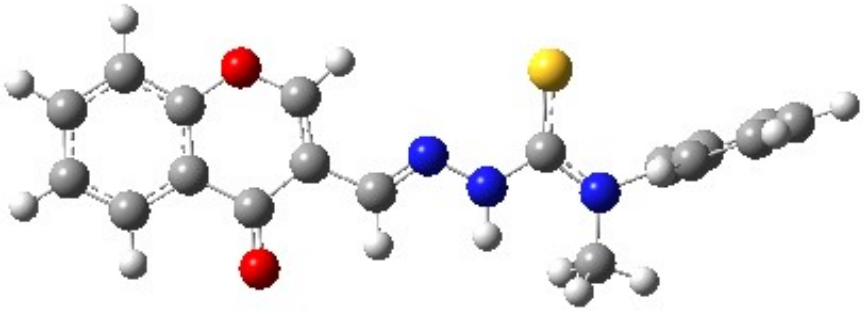

Fig.-1: Optimized Molecule of the Ligand

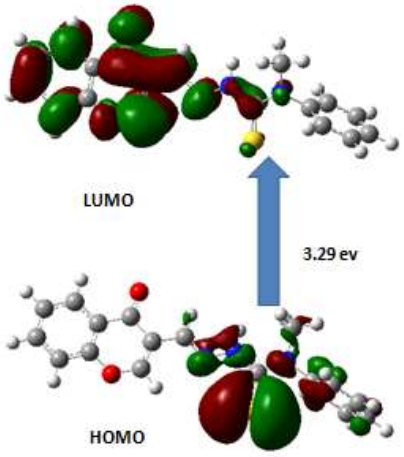

Fig.-2: HOMO- LUMO orbitals, the Corresponding Energy Gap of Ligand

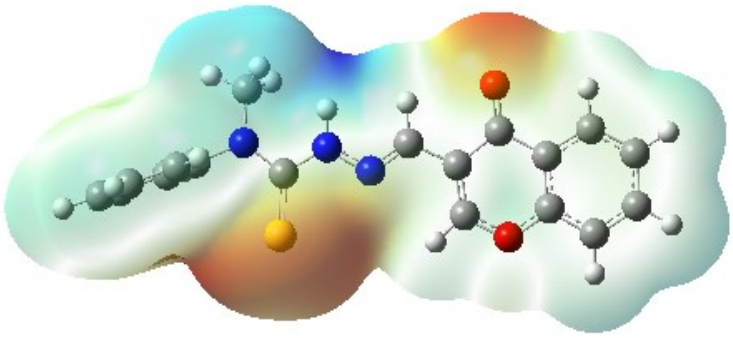

Fig.-3: MEP surface of Ligand

Table-2: Global Descriptive Parameters

Global Descriptive Parameters			
Homo	-5.4089	Softness ζ	0.6078
Lumo	-2.1187	Chemical potential μ	-3.7638
Vertical Ionisation energy I	5.4089	Electronegativity	3.7638
Vertical Electron affinity A	2.1187	Global electrophilic index ω	4.3056
Hardness η	1.6451		

Insilico Screening of Some Drug Designing Parameters

The Molecular weight of the compound is found to be 337g/mol (less than 500). The compound is orally bioavailable as its logP value is 2.77. The number of hydrogen bond donors and hydrogen bond acceptors is 1 (less than 5), and 3 (less than 10), respectively. It is in agreement with the extensions to Lipinski's rule of five, with the polar surface area given by 89.93Å^2 (less than or equal to 140Å^2) and the number of

rotatable bonds equal to 5(less than or equal to 10). Lipinski's rule of five is obeyed by the compound, thereby guaranteeing good oral bioavailability.40[40] The computed pharma-core data showing its oral bioavailability are given in Table-S1. ADME properties, drug-likeness, and medicinal chemistry friendliness were calculated with SwissADME and are summarized in Table-S2. The lipophilic nature of the compound was calculated by taking the means of the five predicted values, ie Consensus logP which is equal to 2.99. ESOL model evaluated the moderate water solubility of the molecule as -4.09 whereas the Ali model, and SILICOS-IT, showed -4.73, and -6.12, respectively. But gastrointestinal absorption is found to be high, allowing for oral administration. The molecule is not a Permeability glycoprotein (Pgp) substrate, the active efflux transporter and Blood-Brain Barrier (BBB) are permeable. It displays inhibition towards CYP2C19, CYP1A2, CYP3A4, and CYP2C9 enzymes whereas acts as a non-inhibitor for the CYP2D6 enzyme. A bioavailability score of 0.55 further confirms the high potential of the ligand as a drug-like molecule.[40] The medicinal chemistry friendliness parameter indicates moderately easy availability to synthesis.[40]

Docking studies

The ligand was docked into the protein binding sites. A few ligand poses were generated for docking calculation. The least negative XP g-score (negative value) indicates the best binding score for the ligand with protein.30,40[30,40] The compound made three hydrogen bonding interactions with the residues, Arg 330, Glu 334, Asp 271, and Ser 263 docked deeply into the active site region of the ribonucleoside diphosphate reductase M-2 subunit. The compound docked deeply into the active site region of DNA methyl transferase, making interactions with the residues Glu 660, Phe 636, Gly 703, Trp 889, and Ser 263. It docked deeply into the histone deacetylase 8 active site region and interacted with the residues His 143, He 180, Asp 178, Asp 101, Gly 151, and Ser 263 via hydrogen bonds. The docking outcomes are reported in Table-3. Figure-4 shows the docked pose of the inhibitor inside the binding pockets of the proteins (a) (PDB ID: 2UW2) (b) (PDB ID: 2QRV) and (c) (PDB ID: 1T69).

Table-3: Glide Score and Glide Energy of Ligand

Protein	Glide score	Glide energy
Ribonucleoside diphosphate reductase M2subunit PDB ID 2UW2	-6.438	-43.039
DNA Methyl transferase (PDB ID 2QRV)	-6.222	-45.642
Histone deacetylase 8 (PDB ID 1T69	-8.148	-34.238

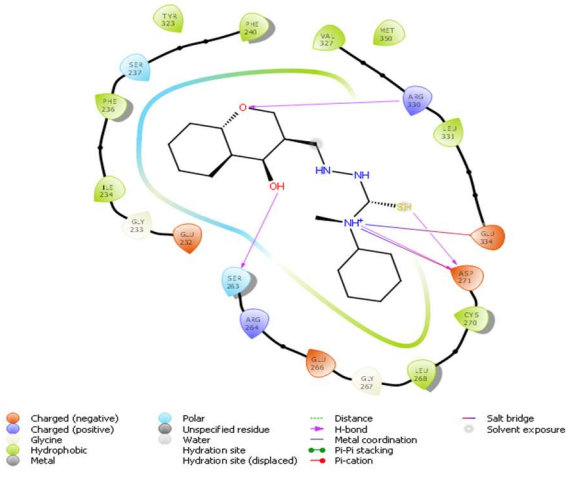

(a)

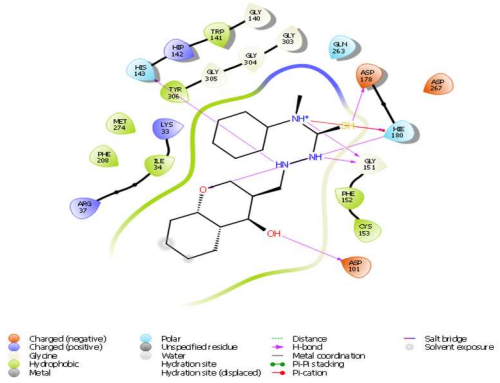

(b)

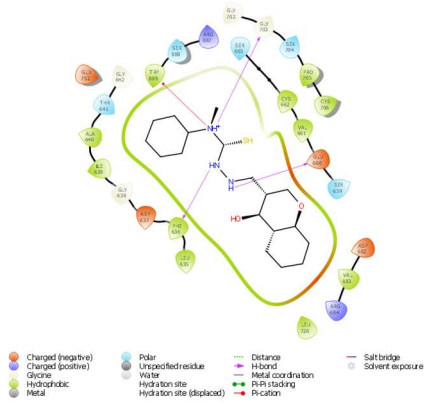

(c)

Fig.-4: Docked Pose of the Inhibitor, Inside the Binding Pockets of Proteins (a) (PDB ID: 2UW2) (b) (PDB ID: 2QRV) and (c) (PDB ID: 1T69)

CONCLUSION

In this investigation, a novel 3-formylchromone thiosemicarbazone and five metal complexes were synthesized and characterized. In complexes, the ligand was coordinated as monoanionic or neutral forms. CHNS analysis, spectroscopy, magnetic moment, and TG/DTG studies were used to propose the structures of complexes. Density Functional Theory (DFT) calculations generated HOMO-, LUMO- and the energy gap is found to be 3.29 ev. The ligand may be a possible inhibitor for the Histone deacetylase 8 (PDB ID 1T69) proteins, according to a molecular docking study. The compound's *insilico* screening for an effective drug was successful. We expect that these results will provide useful information to researchers and motivate them to explore further in this field. However, these computational predictions can be confirmed by in vitro and in vivo analysis.

ACKNOWLEDGMENTS

The authors are indebted to SAIF, Cochin University of Science and Technology, Kochi, Kerala, India for CHNS analyses and NMR spectral analysis. One of the authors (K. G) is thankful to the University Grants Commission Bangalore, for financial assistance in the form of a FDP fellowship.

CONFLICT OF INTERESTS

The authors declare that they have no known competing financial interests or personal relationships that could have appeared to influence the work reported in this paper.

AUTHOR CONTRIBUTIONS

All the authors contributed significantly to this manuscript, participated in reviewing/editing and approved the final draft for publication. The research profile of the authors can be verified from their ORCID ids, given below:

K. G. Sangeetha https://orcid.org/0000-0001-9741-0679
K. K. Aravindakshan https://orcid.org/0009-0007-0349-3241

Open Access: This article is distributed under the terms of the Creative Commons Attribution 4.0 International License (http://creativecommons.org/licenses/by/4.0/), which permits unrestricted use, distribution, and reproduction in any medium, provided you give appropriate credit to the original author(s) and the source, provide a link to the Creative Commons license, and indicate if changes were made.

REFERENCES

1. R.A. Finch, M.C. Liu, A.H. Cory, J.G. Cory, A.C. Sartorelli, *Advances in Enzyme Regulation*, **39**, 3(1999), https://doi.org/10.1016/s0065-2571(98)00017-x
2. W. Antholine, J. Knight, H. Whelan, D.H. Petering, *Molecular Pharmacology*, **13**, 89 (1977)
3. C. M. Nutting, C. M. L. Van Herpen, A. B. Miah, *Annals of Oncology*, **20**, 1275 (2009) https://doi.org/10.1093/annonc/mdn775
4. B. K. Kaymakcioglu, S. Rollas, *Farmaco* **57**, 595(2002), https://doi.org/10.1016/s0014-827x(02)01255-7
5. B. Ma, B. C. Goh, E. H. Tan, *Investigational New Drug Application*, **26**, 169(2008), https://doi.org/10.1007/s10637-007-9085-0
6. S. R. Zhang, A.D. Sherry, *Journal of Solid State Chemistry*, **17**,138 (2003)
7. W.Huang, M.-Z Liu, Y. Li, Y. Tan, G.-F Yamg., *Bioorganic & Medicinal Chemistry*, **15**, 5191(2007), https://doi.org/10.1016/j.bmc.2007.05.022
8. D. Miller, S.Wang , J. Reid , W. Xie , B. Gauvin , M. Kelley, D.G. Sarup, J. Sawutz, M. Miski, R. E. Dolle, C. R. Faltynek, *Drug Development Research*, **34**, 344(1995)
9. S. Selvamuruga, R. Ramachandran , P. Vijayan, R. Manikandan, G. Prakash, P. Viswanathamurthi, K. Velmurugan , R. Nandhakumar and A. Endo, *Polyhedron*, **107** , 57(2016); (*b*) P. Li , M. Niu , M. Hong , S. Cheng and J. Dou, *Journal of Inorganic Biochemistry,* **137**, 101(2014), 10.1016/j.jinorgbio.2014.04.005
10. Y. Li, Z.-Y. Yang, and J.-C. Wu, *European Journal of Medicinal Chemistry*, **45**, 5692 (2010)
11. S. Küçükgüzel, S. Rollas, I. Küçükgüzel, M. Kiraz, *European Journal of Medicinal Chemistry,* **34**, 1093 (1999)
12. Palakuri Kavitha, K. Laxma Reddy, *Bioinorganic Chemistry and Applications*, **2014**, 2014, https://doi.org/10.1155/2014/568741
13. D.-D. Qin, Z.-Y. Yang, and B.-D. Wang, *Spectrochimica Acta A: Molecular and Biomolecular Spectroscopy*, **68**, 912 (2007).
14. J.D. Durrant, J.A. Mccammon, .*BMC Biology,* **9**,71(2011), https://doi.org/10.1186/1741-7007-9-71
15. J. J. Tan, X. J. Cong, L. M. Hu, C. X. Wang, L. Jia, X. J. Liang, *Drug Discovery Today*, **15**,186 (2010)
16. K.G. Sangeetha, K.K. Aravindakshan, *Journal of Molecular Structure*, **1150**,135(2017), https://doi.org/10.1016/j.molstruc.2017.08.078
17. S. Balasubramanian, J. Ramos, W. Luo, M. Sirisawad, E. Verner, J.J. Buggy, *Leukemia* **22 (5)**, 1026(2008)
18. G. Nocentini, *Critical Reviews in Oncology/Hematology* , **22(2)**, 89 (1996)
19. M. Ehrlich, *Oncogene* **21**, 5400 (2002)
20. A. Bird, *Genes & Development*, **16**, 6 (2002), https://doi.org/10.1101/gad.947102
21. P. A. Jones, S. B. Baylin, *Nature Reviews Genetics*, **3**, 415(2002), https://doi.org/10.1038/nrg816
22. K. D. Robertson, *Nature Reviews Genetics*, **6**, 597(2005), https://doi.org/10.1038/nrg1655
23. A. Ricca, C.W. Bauschlicher *The Journal of Physical Chemistry A*, **99**, 9003(1995), https://doi.org/10.1021/j100022a010
24. A.D. Becke, *The Journal of Physical Chemistry A*., **98**, 5648(1993), https://doi.org/10.1063/1.464913
25. A.P. Scott, L. Radom, The Journal of Physical Chemistry A, **100**, 16502 (1996) https://doi.org/10.1021/jp960976r
26. A. Daina, O. Michielin, *Journal of Chemical Information and Modeling*, **54**, 3284 (2014)
27. C.A. Lipinski, *Advanced Drug Delivery Reviews*, **46**,3 (2001)

28. G.A. Kaminski, R.A. Friesner, J. Tirado-Rives, W.L. Jorgensen, *The Journal of Physical Chemistry B*, **105**, 6474(2001)
29. J.J. Blessy, D.J.S. Sharmila, *Journal of Biomolecular Structure and Dynamics*, **33(5)**, 1126(2015)
30. K.G. Sangeetha, K.K. Aravindakshan, *Results in Chemistry,* **4**, 100453(2022), https://doi.org/10.1016/j.rechem.2022.100453
31. A. P. Mishra and D. K. Mishra, *International Journal of Pharma and Bio Sciences*, **2**, 430 (2011)
32. R.M. Issa, A.M. Khedr, H.F. Rizk *Spectrochimica Acta Part A: Molecular and Biomolecular Spectroscopy*, **62**, 621(2005), https://doi.org/10.1016/j.saa.2005.01.026
33. M.H. Habibi, M. Montazerozohori, A. Lalegani, R.W. Harrington, W. Clegg, *Journal of Fluorine Chemistry*, **127**,769 (2006), http://dx.doi.org/10.1016/j.jfluchem.2006.02.014
34. K. Ramakrishna Reddy, K. Madhusudhan Reddy, K. N. Mahendra, *Indian Journal of Chemistry,* **45A**,377(2006)
35. A.K.Mukherjee, P.Ray, *Journal of the Indian Chemical Society*, **32**, 633 (1955)
36. L. Sacconi, R. Cini, *Annali di Chimica (Italy)*, **42** 723 (1952)
37. K. P Deepa. Ph.D. Thesis, University of Calicut, 1998.
38. D. Matoga, J. Szklarzewicz, R. Grybos, K. Kurpiewska, W. Nitek, *Inorganic Chemistry*, **50**, 3501(2011)
39. S. Bootwala, M. Tariq, S. Somasundaran, K. Aruna, *International Journal of Pharma and Bio Sciences,* **3**, 345(2013)
40. K.G. Sangeetha, K.K. Aravindakshan, *Results in Chemistry,* **4**, 100534(2022), https://doi.org/10.1016/j.rechem.2022.100534

[RJC-8352/2023]